Jordanian Journal of Engineering and Chemical Industries

Print ISSN: 2616 - 9584 Online ISSN: 2617 - 720X

# Pollution Characteristics and Ecological and Human Health Risk Assessment of Toxic Elements in Fallout Dusts of Ma'an District Schools

**Mohammad Batiha[*1)], Leema Al-Makhadmeh[2)], Saleh Rawadieh[1)], Marwan Batiha[1)], Muawia Alqasaimeh[3)], Aseel Alhasan[1)], Aseel Atalah[1)], Maria Abo Aljoud[1)], and Salah Nasralah[1)]**

*[1)]Chemical Engineering Department, Faculty of Engineering, Al-Hussein Bin Talal University, Ma'an, 71111, Jordan.*

*[2)]Environmental Engineering Department, Faculty of Engineering, Al-Hussein Bin Talal University, Ma'an, 71111, Jordan.*

*[3)]Chemistry Department, Faculty of Science, Al-Hussein Bin Talal University, Ma'an, 71111, Jordan.*

**Abstract**

The main goals of this paper were to (i) analyze the fallout dust deposits collected from 16 schools in the Ma'an district in Jordan and study their pollution characteristics and (ii) assess the ecological and human health risk of potentially toxic elements (PTEs) exposure to these dusts. Elemental and mineralogy analyses were conducted using X-ray fluorescence and diffraction techniques. The most abundant major elements in the dust were Ca, Si, Fe and Al, while the main minerals were carbonate and silicate indicating the detrital sedimentary origin of the dust. The pollution level was assessed using the enrichment factor, contamination factor, geo-accumulation index, the Nemerow integrated pollution index and pollution load index, which were in the order of Zn>Pb>Cu>Cr>V>Mn=Fe. The potential ecological risk results showed a very low ecological risk. For children and adults, both carcinogenic and non-carcinogenic health risks related to ingestion, dermal contact and inhalation of fallout dust were assessed.

**Paper type**: Research paper

**Keywords**: Potentially toxic elements, Jordan, school, risk assessment, fallout dust.

**Citation**: Mohammad Batiha, Leema Al-Makhadmeh, Saleh Rawadieh, Marwan Batiha, Muawia Alqasaimeh, Aseel Alhasan, Aseel Atalah, Maria Abo Aljoud, and Salah Nasralah "Pollution Characteristics And Ecological And Human Health Risk Assessment of Toxic Elements in Fallout Dusts of Ma'an District Schools", Jordanian Journal of Engineering and Chemical Industries, Vol. 7, No.1, pp: 23-40 (2024).

## Introduction

Human health is affected by many pollutants emitted into environmental media (air, water, soil), which they are originated from natural and anthropogenic sources. Such undesirable effects can be classified as direct (i.e., affecting man) or indirect (i.e., being mediated via resource organisms or climate change) (Rai 2016). One class of these pollutants is toxic heavy metals (HMs), which are considered potentially toxic elements (PTEs). There are many sources of PTEs in air compartments, such as fallout dust, vehicle exhaust and traffic emission, industrial plants, city construction, contaminated soils, atmospheric dispersion, earth crust, mining, urban runoff, and sewage discharge (Manno *et al.*, 2006). HMs toxicity is a major threat and causes several health risks and is considered harmful for the human body and its proper functioning. They cause various disorders and excessive damage due to oxidative stress induced by free radical formation (Jaishankar *et al.*, 2014). Also, they accumulate in the body tissues and threaten their health. In addition, they affect the immune system, the central nervous system, the circulatory system and other organs. After long contact time, they also may cause cancer (Gope *et al.*, 2017; Shabbaj *et al.*, 2018). PTEs enter human beings by inhalation, ingestion and dermal contact; oral ingestion is the most critical exposure pathway (Li *et al.*, 2017). In addition, PTEs adversely affect the ecological environment (Chen *et al.*, 2018; Saleem *et al.*, 2018).

Metals exist naturally in the earth's crust with different spatial variations of surrounding concentrations (Khlifi *et al.*, 2013). Soils are the major sink for metal contaminants (Kirpichtchikova *et al.*, 2006). Dust particles with size≤50 μm are entrained with air and meteorological parameters such as wind direction and speed affect dust particles movement.

* Corresponding author: E-mail: mbatiha@ahu.edu.jo ORCID: https://orcid.org/0000-0003-2898-0584

Received on March 7, 2024. Accepted on March 30, 2024.

*Jordanian Journal of Engineering and Chemical Industries* (JJECI), Vol.7, No.1, 2023, pp: 23-40. Revised: March 29, 2024.

Most searches study extensively Cd, Cu, Pb, Zn, Ni, As, and Hg concentrations. Since Cd, Cu, Pb and Zn appear in gasoline, car components, oil lubricants, and industrial and incinerator emissions, they are considered as good indicators of soil contamination (X. Li *et al.*, 2001). Heavy metal from anthropogenic sources mostly concentrates in the fine grain-size fraction. Fine grains have a larger surface area resulting in higher cation exchange capacity and subsequent metal adsorption (Horowitz and Elrick 1986; Yeats and Bewers 1982). Many workers reported an association of heavy metals with finer size fractions (Robertson and Taylor 2007; Singh *et al.*, 1999). Potgieter-Vermaak *et al.*, (2012) suggested to characterize the molecular composition of the fine fraction of non-exhaust emission dusts. These particle-bound airborne transition metals might produce reactive oxygen species in the lung tissue of children and adults with oxidation stress potential of particles higher than that of diesel exhaust particle emission. Dry or wet sieving methods can be used for the size fractionation of sediment grains. De Groot *et al.*, (1982) found that dry sieving is faster and better than wet sieving, it can also adequately assess metal content variation in different sediments.

Literature is saturated with studies on exhaust emissions and their ecological and human health risks. Research on exhaust emissions has been conducted over the past 50 years, which resulted in technological advances causing reduced emissions from combustion engines (Al-Makhadmeh *et al.*, 2018; Al-makhadmeh *et al.*, 2017; Boyle 1996; Pant and Harrison 2013; Sydbom *et al.*, 2001). In contrast, there is a limited number of studies on non-exhaust emission sources that consider both ecological and human health impacts (Adamiec and Jarosz-Krzemińska 2019; Amato *et al.*, 2014). At the same time, there is a lack of technological advances or legislative measures that could reduce non-exhaust emissions. Therefore, this study aims to (i) characterize the fine grain-size fractions of the fallout dust deposits collected from 16 schools in the Ma'an district in Jordan and identify their pollution characteristics and (ii) assess the ecological and human health risk of PTEs exposure to these dusts. In addition, one of the intents of this work is to help the decision-makers implement the proper measures that could improve the environmental conditions in the study area. Elemental and mineralogy analyses are conducted using X-ray fluorescence (XRF) and X-ray diffraction (XRD) techniques. For a better understanding of the origin and physical and chemical properties of dust, a particle size distribution test is conducted. Pollution level is assessed using enrichment factor, contamination factor, geo-accumulation index, the Nemerow integrated pollution index and pollution load index. The potential ecological risk is addressed using the risk factor suggested by Hakanson (1980). For children and adults, both carcinogenic and non-carcinogenic health risks related to ingestion, dermal contact and inhalation of fallout dust are assessed using hazard quotient and hazard index.

# 1 Materials and Methods

## 1.1 Study area

Ma'an governorate includes four districts, namely Ma'an, Petra, Shobak and Huseiniya. It covers the largest area among the 12 governorates of the Hashemite Kingdom of Jordan with a total surface area of 32832 km$^2$ (37% of the total area of Jordan) and has relatively low population density of 5.2 people per km$^2$. The estimated population in Ma'an governorate was 179300 at end-year 2020, which accounts for 1.7% of the total population in Jordan. It is located 220 km southwest of the capital Amman (**Figure 1**). Ma'an governorate is located at latitude 30°10′ N and longitude 35°47′ E within the world solar belt with almost 300 sunny days per year. Among the four districts, Ma'an district was selected as a study area. The estimated population in Ma'an district is 99320 at end-year 2020 (Statistics 2020). It lies 1069 m above sea level and is characterized by an arid climate with a mean annual temperature of 18.8°C, mean annual rainfall of 10.1 mm, and mean annual relative humidity of 47.8% (Meteorology 2017).

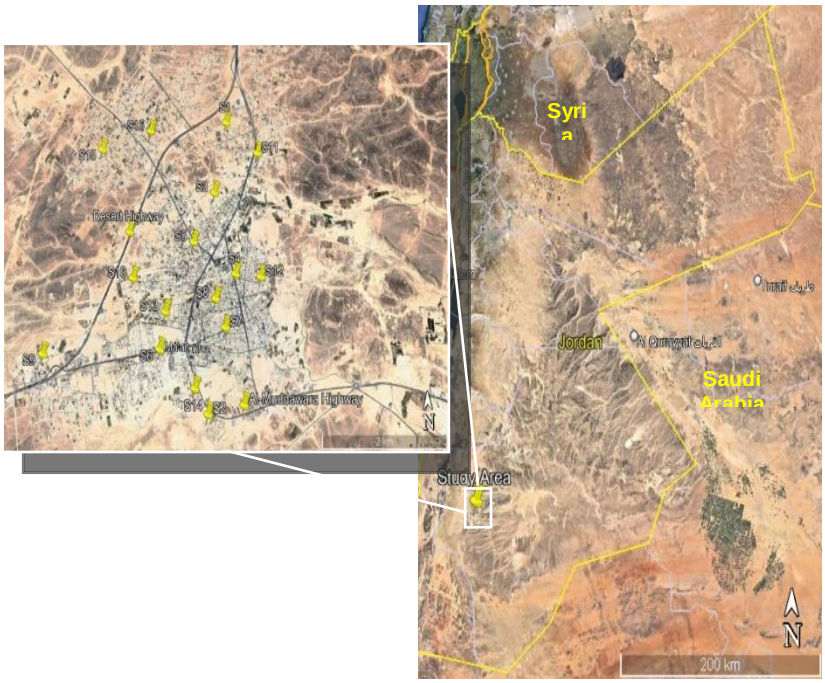


**Fig. 1** Map showing the study area and sampling sites (Source: Google Earth).

### 1.2 Sampling

As listed in **Table 1** and shown in Fig. 1, 16 fallout dust samples were collected in April 2022 from different schools located within the Ma'an district. To avoid re-suspension of very fine dust during sampling, samples were carefully collected using plastic brushes and dustpans. Each sample was made from five fallout dust mixtures collected from the various external impervious surfaces of each school. The samples were air dried at 40°C and then screened through a 2 mm sieve to remove any extraneous materials (stones, debris, waste plastic, leaves, hair, etc.). Then, they were kept in self-sealing bags and stored in a refrigerator at 4°C until the analysis.

### 1.3 Particle-size distribution

For a better understanding of the origin and physical and chemical properties of dust, a particle size distribution test was conducted. Dust samples were screened using dry vibratory sieving and fractionated into the following eight grain-size ranges: 180–200, 150–180, 125–150, 106–125, 75–106, 38–75 and <38μm.

### 1.4 Dust characterization methods

In this study, the pan fractions (*i.e.* dust with grain size <38μm) were selected for elemental and mineral analysis; because dust with finer size fraction is easy to inhale, ingest and adsorb through the skin. Also, in the grain-size fraction <63μm, the concentrations of heavy metals are 1–3 times higher than fractions with higher sizes (Robertson and Taylor 2007; Singh 2011). Dust samples were characterized for their chemical (elemental) composition using XRF (EXD-7000, Shimadzu Corporation, Japan). Minerals are best determined using XRD technology, which is phase phase-sensitive technique compared with XRF which is chemically sensitive. Hence, mineralogy analysis was conducted using XRD (LabX XRD-6100, Shimadzu Corporation, Japan). Dusts were crushed in agate mortar to a very fine powder. A computer-controlled Hiltonbrooks® generator with a Philips® PW 1050 diffractometer with an automatic divergence slit, and Cu anode producing X-rays of wavelength λ=1.54056 Å was used. The diffractometer was operating at voltage 40kV and current 20 mA, and automatic routines allowed scanning for values 2θ from 10° to 90° using a step size of 0.02° and scan speed of 2°/min. Phases were identified using the X'Pert High Score database with PDF02. We performed the analysis in triplicate and used the mean. These analyses were performed at the scientific research lab at Al-Hussein Bin Talal University, Jordan.

**Table 1** Sampling sites with their geographic coordinates

| Sample ID | School Name | School Coordinates | |
|---|---|---|---|
| | | Latitude | Longitude |
| S1 | King Abdullah II School for Excellence | 30°13'06"N | 35°44'01"E |
| S2 | Al-Hussein Bin Talal Applied School | 30°11'03"N | 35°43'40"E |
| S3 | Nusseibeh Bint Ka'ab Al-Mazniyeh Secondary School | 30°12'33"N | 35°43'50"E |
| S4 | Ma'an Secondary School for Girls | 30°11'58"N | 35°43'59"E |
| S5 | Ma'an Comprehensive Secondary School for Girls | 30°12'13"N | 35°43'34"E |
| S6 | Al-Najah Road School and Kindergerten | 30°11'29"N | 35°43'12"E |
| S7 | Ma'an Basic School | 30°11'40"N | 35°43'47"E |
| S8 | Palestine Primary School | 30°11'41"N | 35°43'55"E |
| S9 | Al Baraa Bin Azeb School | 30°11'30"N | 35°41'55"E |
| S10 | Osama Bin Zaid School | 30°11'58"N | 35°42'54"E |
| S11 | Deaf and physical disability school | 30°12'51"N | 35°44'22"E |
| S12 | Khalil Ibn Ahmed Al-Farahidi School | 30°11'56"N | 35°44'19"E |
| S13 | Mohammed Khattab School for Boys | 30°11'43"N | 35°43'17"E |
| S14 | Omar Ibn Al-Khattab School | 30°11'13"N | 35°43'31"E |
| S15 | Abdul Rahman Bin Auf School | 30°12'55"N | 35°42'38"E |
| S16 | Pearl School and Kindergarten | 30°13'03"N | 35°43'11"E |

### 1.5 Pollution level assessment methods

#### 1.5.1 Enrichment factor (*EF*)

The enrichment factor (*EF*) is an important indicator that is widely used to assess dust contamination (enrichment) and to distinguish between natural and anthropogenic sources. Among the common reference elements used in the literature (i.e. Fe, Zr, Al, Ti and Sc), Fe is an immobile element in the environment that has insignificant anthropogenic sources and is used to normalize heavy metals contaminants (Loska *et al.,* 2004). According to Taylor and McLennan (1981; 1995), the average crustal abundance of Fe, Cu, Pb, Zn, Cr, Mn, V and Ni are 58300, 60, 10, 70, 55, 1100, 175 and 30mg/kg, respectively. According to Zoller *et al.,* (1974), *EF* is calculated as:

$$EF = \frac{\left(\frac{C_i}{C_R}\right)_{\text{sample}}}{\left(\frac{C_i}{C_R}\right)_{\text{background}}} \quad (1)$$

where $(C_i/C_R)_{sample}$ and $(C_i/C_R)_{background}$ are the ratios of the concentrations of heavy metal in the dust sample ($C_i$,mg/kg) to the background concentration of earth crust reference metal ($C_R$, mg/kg), respectively. The following *EF* categories are used to estimate the degree of metal pollution: depletion to minimal (*EF*<2), moderate (2≤*EF*<5), significant (5≤*EF*<20), very high (20≤ *EF*<40), and extremely high (*EF*≥40). *EF* is only significant if *EF*>5, since enrichment up to 5 could be referred to as the difference in composition between local dust and that of the earth crust reference metal used.

### 1.5.2 Index of geo-accumulation ($I_{geo}$)

Muller (1969) suggested the index of geo-accumulation ($I_{geo}$) in bottom sediments, which was after that widely used to assess the contamination of heavy metals in street dust by comparing the concentrations of heavy metal in dust samples to the background concentrations. It can be calculated as follows:

$$I_{geo} = \log_2\left(\frac{C_i}{1.5B_i}\right) \quad (2)$$

where $C_i$ is the concentration of the metal in fallout dust, and $B_i$ is the crustal average background concentration of the heavy metal. The following $I_{geo}$ categories are used: unpolluted environment (*Igeo*≤0), unpolluted to moderately polluted (0<*Igeo*≤1), moderately polluted (1<*Igeo* ≤2), moderately to strongly polluted (2<*Igeo*≤3), strongly polluted (3<*Igeo*≤4), strongly to extremely polluted (4<*Igeo*≤5), and extremely polluted (*Igeo*>5).

### 1.5.3 Pollution assessment indexes

Hakanson (1980) introduced the contamination factor (*CF*) as a tool to assess the level of single *PTE* contamination in fallout dust samples:

$$CF = \frac{C_{i\ sample}}{C_{i\ background}} \quad (3)$$

where $C_{i\ background}$ is the heavy metals background concentration in the earth's crust and $C_{i\ Sample}$ is the heavy metals concentration in fallout dust samples. *CF* interpretation is as follows (Tomlinson *et al.*, 1980): low polluted (*CF*≤1), moderately polluted (1<*CF*≤3), considerably polluted (3<*CF*≤6) and highly polluted (*CF*>6).

The Nemerow Integrated Pollution Index (*NIPI*) takes into account the effect of all considered *PTEs* and their effect on the maximum *CF*. It is used to estimate the pollution level of a single heavy metal, taking into account all sites in the study area (Cheng *et al.*, 2007; He *et al.*, 2016; Yesilkanat and Kobya 2021) and is calculated as follows:

$$NIPI_i = \sqrt{\frac{(CF_i)^2_{max} + (CF_i)^2_{ave}}{2}} \quad (4)$$

where $CF_{i,max}$ and $CF_{i,ave}$ are the maximum and mean *CF* values of ith *PTE* in all studied sites, respectively. The *NIPI* interpretation is as follows: unpolluted (*NIPI*≤0.7), warning limit of pollution (0.7<*NIPI*≤1), low polluted (1<*NIPI*≤2), moderately polluted (2<*NIPI*≤3) and strongly polluted (*NIPI*>3).

Tomlinson *et al.*, (1980) introduced the pollution load index (*PLI*) which indicates the cumulative pollution load from all studied heavy metals at each site. *PLI* for any site is:

$$PLI_{\text{site}} = \sqrt[n]{CF_1 \times CF_2 \times \ldots \times CF_{\text{n}}} \quad (5)$$

and for the whole studied zone:

$$PLI_{\text{zone}} = \sqrt[m]{PLI_{\text{site},1} \times PLI_{\text{site},2} \times \ldots \times PLI_{\text{site,m}}} \quad (6)$$

where *n* and *m* are the number of species and sites considered, respectively. *PLI* is divided into two main categories: baseline level of pollution (*PLI*=1) and polluted site/zone (*PLI*>1).

### 1.6 Ecological risk assessment

The potential ecological risk of *PTEs* was quantitatively assessed using the risk factor (*ERF*) suggested by Hakanson (1980) as follows:

$$ERF_i = \mathrm{TR_i} \times CF_\mathrm{i} \tag{7}$$

where $\mathrm{TR_i}$ is the toxic-response factor for ith PTE (e.g., $TR_{Pb}$=$TR_{Cu}$=$TR_{Ni}$=5; $TR_{Cr}$=$TR_V$=2; $TR_{Zn}$=$TR_{Mn}$=1). *ERF* is categorized as follows: low potential ecological risk ($ERF_i$<40), moderate (40≤$ERF_i$<80), considerable (80≤$ERF_i$<160), high (160≤$ERF_i$<320) and very high ($ERF_i$≥320). The potential ecological risk index (*ERI*) for the region is the sum of all $ERF_i$:

$$ERI = \sum_{i=1}^{n} (ERF_i) \tag{8}$$

The *ERI* interpretation is as follows: low potential risk (*ERI*<150), moderate (150≤*ERI*< 300), considerable (300≤*ERI*<600) and very high (*ERI*≥600).

### 1.7 Health risk assessment

In this study, both carcinogenic and non-carcinogenic health risk assessments were considered by utilizing the methods suggested by the United States Environmental Protection Agency (USEPA 1989, 1996, 2002, 2007, 1993).

#### 1.7.1 Exposure assessment

Human is affected by *PTE*s through three main exposure pathways: ingestion, inhalation and dermal contact. The average daily intake dose (*ADD*, mg/kg-day) of *PTEs* affecting both children and adults are:

$$\mathrm{ADD_{ing}} = \frac{\mathrm{C_i} \times \mathrm{IngR} \times CF \times EF \times \mathrm{ED}}{\mathrm{BW} \times \mathrm{AT}} \tag{9}$$

$$\mathrm{ADD_{inh}} = \frac{\mathrm{C_i} \times \mathrm{InhR} \times EF \times \mathrm{ED}}{\mathrm{P}EF \times \mathrm{BW} \times \mathrm{AT}} \tag{10}$$

$$\mathrm{ADD_{derm}} = \frac{\mathrm{C_i} \times \mathrm{SL} \times \mathrm{SA} \times \mathrm{ABS} \times EF \times \mathrm{ED} \times CF}{\mathrm{BW} \times \mathrm{AT}} \tag{11}$$

The definition of parameters used in Eqs. (9-11) with their default values and units were listed in **Table 2**. Values for these parameters were obtained from USEPA (2001, 2011), Adamiec and Jarosz-Krzemińska (2019), Zhou *et al.,* (2015) and Jordanova *et al.,* (2021).

#### 1.7.2 Non-carcinogenic risk assessment

For the three main exposure pathways mentioned above, the potential non-cancer risk of each *PTE* was assessed via hazard quotient (*HQ*) as follows (Jayarathne *et al.*, 2018; Li *et al.*, 2017):

$$HQ_\mathrm{ing} = \frac{\mathrm{ADD_{ing}}}{\mathrm{RfD_{ing}}} \tag{12}$$

$$HQ_\mathrm{derm} = \frac{\mathrm{ADD_{derm}}}{\mathrm{RfD_{derm}} \times \mathrm{GIABS}} \tag{13}$$

$$HQ_\mathrm{inh} = \frac{\mathrm{ADD_{inh}}}{\mathrm{RfD_{inh}}} \tag{14}$$

where $\mathrm{RfD_{ing}}$ is the oral reference dose (mg/kg-day), $\mathrm{RfD_{inh}}$ is the inhalation reference concentration (mg/m$^3$), $\mathrm{RfD_{derm}}$ is the dermal reference dose (mg/kg-day), GIABS is the gastrointestinal absorption factor. Values for these parameters, listed in **Table**

**7**, were obtained from USEPA (2001). According to USEPA (1989), the hazard index (*HI*) is calculated as the sum of the *HQ*s for all assessed *PTE*s. The *HI* interpretation is as follows: *HI*<1: no non-cancer health effects and *HI*>1: non-cancer health risks.

### 1.7.3 Carcinogenic risk assessment

The risk is classified as carcinogenic if the lifetime exposure to dust containing carcinogenic heavy metals might develop any kind of cancer in a human. The carcinogenic risk (*CR*) for ith *PTE* is assessed as follows (Adamiec and Jarosz-Krzemińska 2019; Adimalla 2020; Ferreira-Baptista and De Miguel 2005; Gope *et al.*, 2017; Shabbaj *et al.*, 2018; USEPA 1989):

$$CR_i = \left(\mathrm{ADD_{ing}} \times \mathrm{SF_{ing}}\right)_i + \left(\mathrm{ADD_{inh}} \times \mathrm{IUR}\right)_i + \left(\frac{\mathrm{ADD_{derm}} \times \mathrm{SF_{derm}}}{GIABS}\right)_i \quad (15)$$

where *SF* is the slope factor (kg body per day/mg) and *IUR* is the inhalation unit risk $(\mu g/m^3)^{-1}$. The integrated cancer risk (*CRisk*) is calculated as the sum of *CRi* for all analyzed metals for all exposure pathways. *CR* and *CRisk* have the same classifications as follows: very low cancer risk (*CRi* and $CRisk \leq 10^{-6}$), low cancer risk ($10^{-6} < CRi$ and $CRisk \leq 10^{-4}$), moderate cancer risk ($10^{-4} < CRi$ and $CRisk \leq 10^{-3}$), high cancer risk ($10^{-3} < CRi$ and $CRisk \leq 0.1$), very high cancer risk (*CRi* and $CRisk \geq 0.1$).

**Table 2** Health risk assessment input parameters.

| Parameter | Unit | Definition | Value | |
|---|---|---|---|---|
| | | | Children | Adult |
| BW | kg | Average body weight | 15 | 70 |
| *EF* | days/year | Exposure frequency | 180 | 180 |
| ED | year | Exposure duration | 6 | 24 |
| IngR | mg/day | Ingestion rate of dust | 100 | 50 |
| SL | $mg/cm^2$-h | Skin adherence factor of dust | 0.2 | 0.2 |
| SA | $cm^2$ | Surface area of exposed skin | 2800 | 5700 |
| InhR | $m^3$/day | Inhalation rate of dust | 10 | 20 |
| *CF* | kg/mg | conversion factor | $10^{-6}$ | |
| ABS | unitless | Dermal absorption factor | $10^{-6}$ | |
| PEF | $m^3$/kg | Particle emission factor | $1.316\times10^9$ | |
| AT | day | Average exposure time (non-carcinogens) | AT=ED×365 | |
| | | Average exposure time (carcinogens) | AT=70×365 | |

## 2 Results and Discussion

### 2.1 Particle-size distribution

As was mentioned previously, dust samples were fractionated into seven grain-size fractions with various ranges: 180–200, 150–180, 125–150, 106–125, 75–106, 38–75 and <38µm. The grain-size fractions for the 16 collected samples are shown in **Figure 2**. On an average basis, it was found that 17% of the dust have size <38µm, 29% have size 38–75µm, 18% have size 75–106µm, 9% have size 106–125µm, 9% have size 125–150µm, 7% have size 150–180µm, and 10% have size 180–200µm. The dominant fractions of grain size were 38–75 and 75–106µm followed by <38 and 180–200µm. The average grain size of dust dunes was distributed as 54.3% sand (75-200µm), 28.8% slit (38-75 µm) and 16.9% clay (<38µm). Among the screened samples, the highest volumes for grain size <38µm (clay) were for sites S16, S2, S7, S4 and S3 with percent volumes of 53, 53, 26, 21 and 21%, respectively.

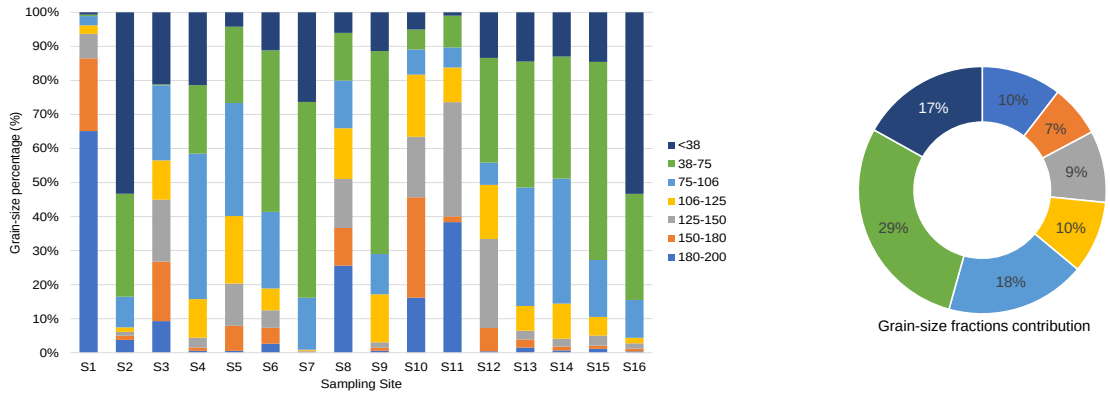


**Fig. 2** Plot of grain-size fractions of dust samples collected from different schools within Ma'an district, Jordan.

## 2.2 Dust Characterization

### 2.2.1 Elemental analysis results

Elemental analysis of dust is essential to identify the sources of pollution and to assess the ecological and health risks of *PTE*s. XRF analysis results showed that the most abundant major elements in the dust were Ca (59%), Si (20%), Fe (10%) and Al (4%), as shown in **Figure 3**, whereas the minor elements were ranked in the order of K>Ti>Mg>Zr>Zn>Sr>Mn>Cl>S>Cu> Cr>P>Pb>V>Ni. The concentrations of Ni were below the detection limit for most sites except for S5, S6, S10 and S11.

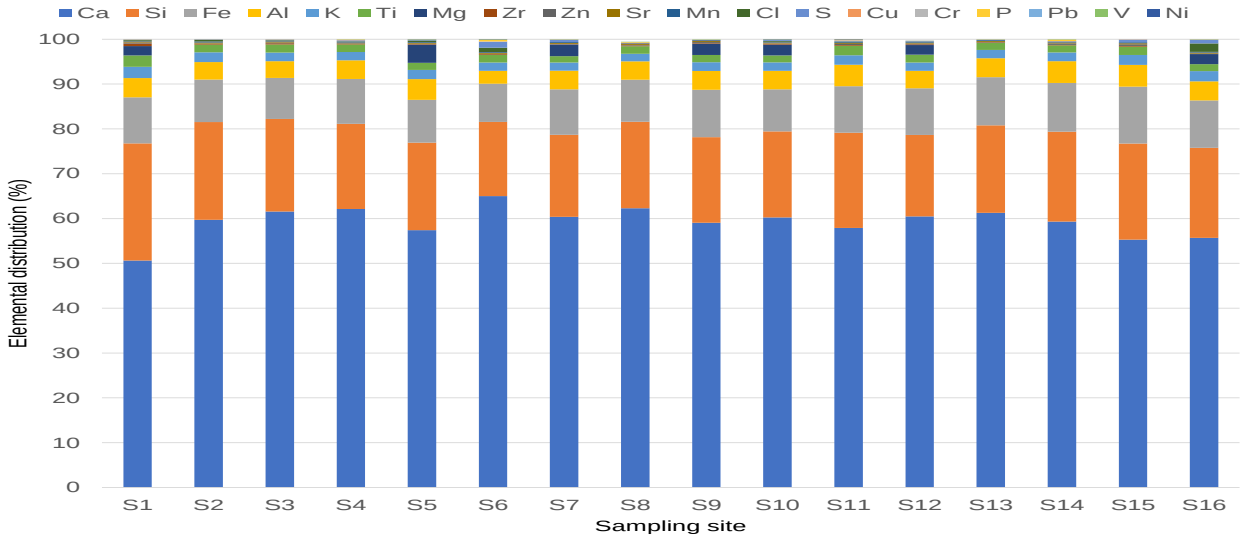


**Fig. 3** Elemental analysis results of all dust samples with grain size <38μm.

For ecological and health risks of fallout dust deposits discussed in the following sections, the following eight *PTE*s with high pollution potential are considered: iron (Fe), copper (Cu), lead (Pb), zinc (Zn), chromium (Cr), manganese (Mn), vanadium (V) and nickel (Ni). The mean concentrations of these *PTE*s in descending order are: Fe(10127.4mg/kg)> Mn(191.4mg/kg)>Zn(160.6mg/kg)>Cu(42.4mg/kg)>V(35.0mg/kg)>Cr(34.7mg/kg)>Pb(11.8mg/kg)>Ni(0.7mg/kg). The obtained mean *PTE*s concentrations in this study were compared with other urban cities around the world, which are listed in Table 3 for Petra (Jordan) (Alsbou and Al-Khashman 2018), Al-Hisa (Jordan) (Hamaiedh and El-Hasan 2011), Fuhis (Jordan) (Banat *et al.*,, 2005), Zerqa (Jordan) (Ghrefat *et al.*,, 2012), Irbid (Jordan) (El-Radaideh and Al-Taani 2018), Jeddah (Saudi Arabia) (Shabbaj *et al.*,, 2018), Riyadh (Saudi Arabia) (Modaihsh *et al.*, 2017), Trabzon (Turkey) (Yesilkanat and Kobya 2021), Dhanbad and Bokaro (India) (Singh 2011), Sistan (Iran) (Rashki *et al.*, 2013), Lahore (Pakistan) (Qadeer *et al.*, 2020), Chittagong (Bangladesh) (Pal and Roy 2021), Urumqi (China) (B. Wei *et al.*, 2009), Xi'an (China) (Pan *et al.*, 2017), Toronto (Canada) (Wiseman *et al.*, 2021), Srednogorie (Bulgaria) (Jordanova *et al.*, 2021) and Gela (Italy) (Manno *et al.*, 2006). As can be seen from **Table 3**, the average concentrations of Fe, Cu, Cr, Mn, V and Ni in the analysed samples were lower than earth crust content, whereas the concentrations of Pb and Zn are 1.20 and 2.30 times higher, respectively.

The average *PTE*s concentrations in the present study were below the average concentrations of all compared cities. Fe concentration in Ma'an is greater than that of Petra and Al-Hisa and lower than that of Jeddah, Zerqa and Srednogorie. Regarding Cu, its concentration in Ma'an is higher than Irbid, Al-Hisa, Sistan, Petra, Lahore, Dhanbad and Bokaro, Riyadh, Trabzon and Chittagong, but it is lower than Zarqa, Xi'an, Urumqi, Toronto, Jeddah, and Gela. Pb concentration in Ma'an is slightly higher than in Sistan and slightly lower than in Al-Hisa, while it is considerably lower than the other cities considered in the comparison. Pb concentration in our study area is slightly higher than Sistan, almost the same as Al-Hisa, and lower than other cities used in the comparison as listed in Table 3; Ma'an is not crowded and there is no heavy traffic volume. Zn concentration in Ma'an is higher than Petra, Irbid, Sistan, Riyadh, Lahore, Dhanbad and Bokaro, Zarqa, and Fuhis, but is lower than Gela, Trabzon, Xi'an, etc. and almost the same as in Chittagong. Mn concentration in Ma'an is lower than in Riyadh but is higher than in Gela, Xia'an, Jeddah, Toronto, Urumqi and Zarqa. For Cr, its concentration in Ma'an is higher than Irbid and Srednogorie, but it is higher than Gela, Riyadh, Trabzon, etc. The concentration of V and Ni in Ma'an is lower than in all ore-mentioned cities, see Table 3. There are clear differences in *PTE*s concentrations between the different cities, this can be a result of the population density, traffic, topography, and meteorology (Shao *et al.*, 2018). Even though, these variations may not represent the real differences between the considered cities (Shabbaj *et al.*, 2018).

The mean *EF* values listed in **Table 4** were in the following order: *n*(12.9)>Pb(6.8)>Cu(4.1)>Cr(3.7)>V(1.2)>Mn(1.0)>Ni(<1.0). The *EF* results show that sites S14 and S15 have very high Zn enrichment with *EF*>20, while significant enrichment for the rest of the sites. Considering all possible emission sources in the study area, the enrichment of Zn in dust samples could be referred to as brake and tyre wear/tear and corrosion of galvanized automobile parts (non-exhaust vehicle emissions); ZnO is known as a vulcanization agent (2–5 mass %) in the tyres manufacturing process and Zn alloy is commonly used in motor vehicles (Baensch-Baltruschat *et al.*, 2020; Li *et al.*, 2017; Men *et al.*,,, 2018; Singh 2011).

**Table 3** Mean *PTE*s concentrations in urban fallout dusts of different cities (mg/kg).

| City (Country) | Cu | Pb | Zn | Cr | Mn | V | Ni |
|---|---|---|---|---|---|---|---|
| Ma'an (Jordan) | 42 | 12 | 161 | 35 | 191 | 35 | 0.7 |
| Petra (Jordan) | 12 | 32 | 25 | | | | |
| Al-Hisa (Jordan) | 4.4 | 13 | 949 | 76 | | | 17 |
| Fuhis (Jordan) | | 62 | 147 | 84 | | | |
| Zerqa (Jordan) | 48 | 58 | 91 | 71 | 936 | | 48 |
| Irbid (Jordan) | 4 | 71 | 46 | 16 | | | 60 |
| Jeddah (Saudi Arabia) | 139 | 141 | 488 | 65 | 551 | 81 | 51 |
| Riyadh (Saudi Arabia) | 27 | 28 | 67 | 44 | 150 | 45 | 20 |
| Trabzon (Turkey) | 29 | 35 | 242 | 45 | | | 27 |
| Dhanbad and Bokaro (India) | 26 | 48 | 78 | 57 | | 57 | 24 |
| Sistan (Iran) | 11 | 10 | 57 | 70 | | 69 | 18 |
| Lahore (Pakistan) | 24 | 44 | 68 | | | | 14 |
| Chittagong (Bangladesh) | 36 | 30 | 160 | | | | 12 |
| Urumqi (China) | 95 | 54 | 295 | 54 | 927 | | 43 |
| Xi'an (China) | 55 | 125 | 269 | 145 | 511 | 70 | 31 |
| Toronto (Canada) | 121 | 63 | 419 | 145 | 784 | 41 | 36 |
| Srednogorie (Bulgaria) | 3483 | 162 | 325 | 30 | | | 19 |
| Gela (Italy) | 189 | 109 | 239 | 41 | 400 | 68 | 34 |
| Minimum | 4.0 | 10.0 | 25.0 | 16.0 | 150.0 | 35.0 | 0.7 |
| Maximum | 3483.0 | 162.0 | 949.0 | 145.0 | 936.0 | 81.0 | 60.0 |
| Mean | 255.6 | 60.9 | 229.2 | 65.2 | 556.3 | 58.3 | 28.4 |

During the sampling period, it was noticed that most schools have installed solar panels on the roofs of schools. Corrosion of galvanized steel tubes used to support these panels might be an additional reason for Zn enrichment in the collected dust. Iron and zinc oxides are among the products of corroded galvanized steel (Colomban *et al.*, 2008). Except for S2, S9, S10 and S16, *EF*s for Pb were in between 5 and 20. The additive of Pb to gasoline in Jordan could be the reason for an increase in vehicle-associated Pb emissions and thus the enrichment of Pb. Most of the selected schools were located within very short distances of medium to high-traffic density roads. Hence, the sources of Zn and Pb in the collected urban fallout dust are mainly derived from traffic emission, although Pb is a persistent element that may enter urban fallout dust via resuspension since it has a long half-life (Chen *et al.*, 2014; Wei and Yang 2010). It was found a moderate enrichment of Cu with *EF*s below 5 in all sites except for S6 and S10. Cu is one of the vehicle tyres components and is used as a brake friction material (Li *et al.*, 2016; Wang *et al.*, 2022).
In Ma'an City, there are many speed bumps in the streets especially in the front of schools which increases braking usage and increases Cu accumulation in fallout dust. Lee and Hopke (2006) reported that higher loading of Cu and Zn might be referred to as diesel vehicles. The trucks transporting phosphate from Al-Sheidia to Aqaba pass through Ma'an city. Also, Ma'an is very close to the desert highway linking northern and southern Jordan which witnessed the movement of trucks in large numbers. Also, the Al-Muddawara highway linking Jordan with Saudi Arabia passes through Ma'an City. The level of traffic flow on these highways might lead to the enrichment of Cu and Zn in the collected dust. Thus, the source of Cu emission in Ma'an City is vehicular traffic. Moderate enrichment of Cr ($5>EF_{Cr}>2$) was found in all sites. Chromium alloys are frequently used as building materials that make construction dust and corrosion of these materials is one of the Cr enrichment in fallout dust (Wang *et al.*, 2022). In the last ten years, Ma'an City witnessed the construction of many government buildings, homes and private shops. Traffic is also responsible for the enrichment of Cr in fallout dust (Manno *et al.*, 2006). Thus, construction and vehicular traffic are the sources of Cr emissions in Ma'an City. Depletion to minimal enrichment of V and Mn were found.

### 2.2.2 Mineralogy analysis

Mineralogical analysis was used to understand the primary source of dust in the Ma'an district. The clay fraction of dust (grain size <38μm) is the most geochemically active fraction from which the dust source is traceable (Ganor and Foner 1996; Idris *et*

*al.*, 2007). The XRD patterns for all dust samples, with grain-size fraction <38μm, are shown in **Figure 4**. They prevailed in a similar mineralogical composition for all samples. Dust mainly contains carbonate and silicate minerals (i.e. calcite and quartz) with traces of clinoferrosilite and clay minerals (dickite). The presence of calcite ($CaCO_3$) and quartz ($SiO_2$) in the analyzed dust samples indicates detrital sedimentary origin (Zarasvandi *et al.*, 2011). These minerals are among the main elements of the earth's crust. Pye (1992) concluded that quartz-rich dust is continental and originates maybe from local areas or short to medium distances, while silicate-rich dust might travel over longer distances. Dickite ($Al_2Si_2O_5(OH)_4$) belongs to the kaolin minerals and kaolinite group. The dickite particles are six-sided and well-formed crystals having diameters of up to 8μm (Mason 1960). It is a usual mineral of fallout dust and is a weathering product of other minerals such as feldspars (Merefield *et al.*, 1995). Clinoferrosilite ($FeSiO_3$) is a diopside type crystalline compound and is an iron ore mineral. Volcanic rock contains $FeSiO_3$ minerals (Dallwitz *et al.*, 1966). Thus, the abundance of volcanic rocks in the Ma'an area could be the source of this mineral in fallout dust. The mineralogy analysis results presented here are in agreement with many other studies in Jordan, in neighbouring countries and the Middle East, such as studies in Jordan (Hamaiedh and El-Hasan 2011), in Iraq (Al-Dabbas *et al.*, 2012; Awadh 2012), in Iran (Hojati *et al.*, 2012; Najafi *et al.*, 2014; Rashki *et al.*, 2013), in Saudi Arabia (Modaihsh *et al.*, 2017) and in Egypt (Shaltout *et al.*, 2016). The mineralogy results are consistent with the elemental composition results discussed earlier.

**Table 4** Enrichment factors for the dust samples in the study area.

| Sample ID | Cu | Pb | Zn | Cr | Mn | V | Ni |
|---|---|---|---|---|---|---|---|
| S1 | 4.4 | 5.3 | 18.9 | 3.1 | 0.9 | 0.2 | - |
| S2 | 5.0 | 4.4 | 5.2 | 3.2 | 1.1 | 0.0 | - |
| S3 | 4.5 | 5.4 | 13.6 | 4.6 | 1.0 | 0.0 | - |
| S4 | 4.3 | 6.5 | 9.6 | 3.5 | 1.0 | 1.4 | - |
| S5 | 4.0 | 9.8 | 9.4 | 4.7 | 1.0 | 1.4 | 1.2 |
| S6 | 6.3 | 7.2 | 9.2 | 4.5 | 1.0 | 2.5 | 0.6 |
| S7 | 4.6 | 6.3 | 8.2 | 3.3 | 1.0 | 1.6 | - |
| S8 | 4.1 | 8.9 | 12.7 | 4.1 | 1.0 | 2.4 | - |
| S9 | 3.5 | 4.2 | 17.0 | 2.7 | 1.0 | 2.2 | - |
| S10 | 5.3 | 4.7 | 6.6 | 4.2 | 1.0 | 1.9 | 0.4 |
| S11 | 4.1 | 9.5 | 18.9 | 4.6 | 0.9 | 0.0 | 0.1 |
| S12 | 0.0 | 11.9 | 13.1 | 2.7 | 0.9 | 0.0 | - |
| S13 | 4.5 | 6.3 | 6.3 | 2.9 | 1.0 | 1.8 | - |
| S14 | 3.3 | 8.4 | 25.7 | 3.4 | 1.2 | 1.4 | - |
| S15 | 3.7 | 6.1 | 25.2 | 3.8 | 1.0 | 0.0 | - |
| S16 | 4.2 | 4.1 | 6.4 | 3.3 | 0.9 | 1.9 | - |
| Minimum | 0.0 | 4.1 | 5.2 | 2.7 | 0.9 | 0.0 | 0.1 |
| Maximum | 6.3 | 11.9 | 25.7 | 4.7 | 1.2 | 2.5 | 1.2 |
| Mean | 4.1 | 6.8 | 12.9 | 3.7 | 1.0 | 1.2 | 0.6 |

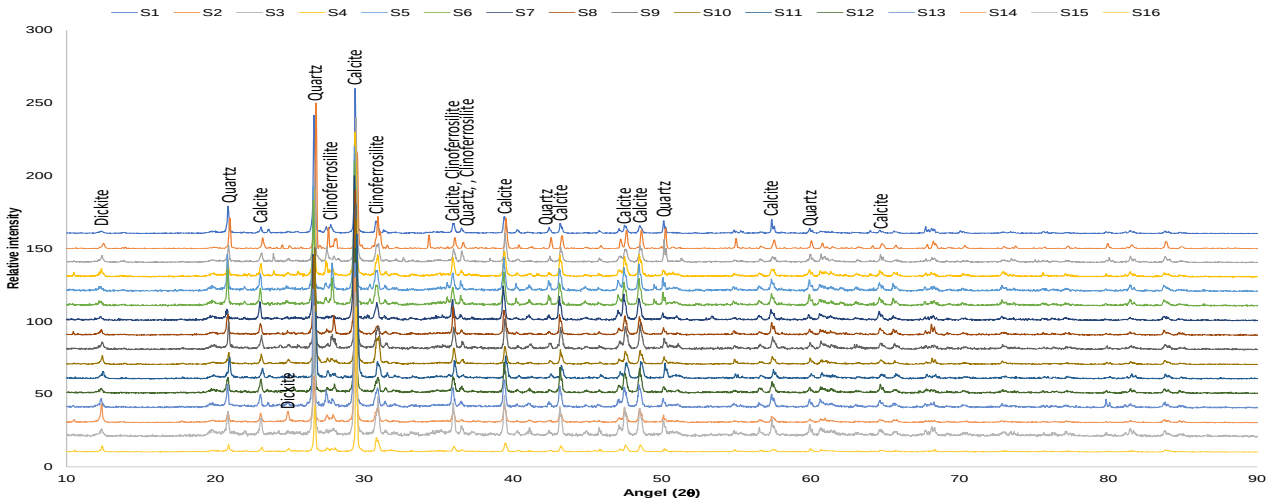


**Fig. 4** XRD analysis results of all dust samples with grain size <38μm.

## 2.3 *PTE*s pollution assessment

### 2.3.1 Geo-accumulation index ($I_{geo}$)

Statistical values of *Igeo* in the study area are listed in **Table 5**. The mean values of *Igeo* were found in the following order: Zn (0.4)>Pb(-0.4)>Cu(-0.9)>Cr(-1.3)>V(-1.8)>Mn(-3.1)=Fe(-3.1). *Igeo* value for Zn falls between 0 and 1 for sites S3, S4, S5, S8 and S12 whereas it falls between 1 and 2 for sites S1, S9, S11, S14 and S15, which indicates that dusts were moderately polluted with zinc. According to *Igeo*, dust is ranked as unpolluted to polluted for Pb in sites S5, S11, S12 and S14. *Igeo* values reveal that the collected dusts were uncontaminated by the rest of the *PTE*s.

**Table 5** Statistical values of the geo-accumulation index (*Igeo*) in the study area.

| Statistical values | Cu | Pb | Zn | Cr | Mn | V |
|---|---|---|---|---|---|---|
| Minimum | -1.3 | -1.1 | -0.8 | -1.6 | -3.4 | -5.4 |
| Maximum | 0.0 | 0.5 | 1.9 | -0.9 | -2.8 | 0.0 |
| Mean | -0.9 | -0.4 | 0.4 | -1.3 | -3.1 | -1.8 |

### 2.3.2 Pollution assessment indexes (*CF* and *NIPI*)

The mean calculated values of *CF* were in the following order: Zn(2.29)>Pb(1.18)>Cu(0.71)>Cr(0.63)>V(0.20)>Mn(0.17)=Fe(0.17). The mean *CF* of Zn and Pb were lower than 3 indicating moderate contamination. For the rest of the *PTE*s, the mean *CF*s were below 1, which indicated low contamination. The contamination factor values for all sampling sites are presented in **Table 6**. As can be seen from this Table, considerable contamination ($3<CF\leq6$) with Zn was found in sites S1, S9, S11, S14 and S15 and moderate contamination in the rest of the sites. Moderate contamination with Pb was found in most sites except for sites S1, S2, S3, S9, S10 and S16 which were ranked as low contamination. The study area was low-contaminated with the rest of the *PTE*s with $CF\leq1$. The *NIPI* values were ranked in the following order: Zn(4.2)>Pb(1.72)>Cu(0.82)>Cr(0.74)>V(0.32)>Mn(0.2)=Fe(0.2). These results indicate that the study area was strongly polluted with zinc, low polluted with lead, warning limit of pollution for Cu and Cr, and not polluted with V, Mn and Fe.

**Table 6** Contamination factors for the dust samples in the study area.

| Sample ID | Cu | Pb | Zn | Cr | Mn | V | Ni |
|---|---|---|---|---|---|---|---|
| S1 | 0.77 | 0.93 | 3.33 | 0.54 | 0.16 | 0.04 | - |
| S2 | 0.81 | 0.71 | 0.84 | 0.51 | 0.18 | 0.00 | - |
| S3 | 0.71 | 0.84 | 2.13 | 0.72 | 0.16 | 0.00 | - |
| S4 | 0.75 | 1.11 | 1.64 | 0.61 | 0.18 | 0.25 | - |
| S5 | 0.66 | 1.62 | 1.54 | 0.77 | 0.17 | 0.23 | 0.20 |
| S6 | 0.92 | 1.04 | 1.34 | 0.66 | 0.14 | 0.37 | 0.08 |
| S7 | 0.80 | 1.10 | 1.43 | 0.58 | 0.17 | 0.29 | - |
| S8 | 0.67 | 1.44 | 2.03 | 0.65 | 0.16 | 0.39 | - |
| S9 | 0.63 | 0.75 | 3.06 | 0.49 | 0.18 | 0.41 | - |
| S10 | 0.85 | 0.76 | 1.07 | 0.67 | 0.17 | 0.30 | 0.06 |
| S11 | 0.73 | 1.69 | 3.37 | 0.82 | 0.17 | 0.00 | 0.01 |
| S12 | 0.00 | 2.13 | 2.34 | 0.48 | 0.16 | 0.00 | - |
| S13 | 0.82 | 1.16 | 1.16 | 0.54 | 0.18 | 0.32 | - |
| S14 | 0.62 | 1.57 | 4.78 | 0.64 | 0.22 | 0.27 | - |
| S15 | 0.81 | 1.32 | 5.48 | 0.83 | 0.21 | 0.00 | - |
| S16 | 0.77 | 0.75 | 1.16 | 0.60 | 0.17 | 0.35 | - |
| Minimum | 0.0 | 0.7 | 0.8 | 0.5 | 0.1 | 0.0 | 0.0 |
| Maximum | 0.9 | 2.1 | 5.5 | 0.8 | 0.2 | 0.4 | 0.2 |
| Mean | 0.7 | 1.2 | 2.3 | 0.6 | 0.2 | 0.2 | 0.1 |

### 2.3.3 Pollution Load Index (PLI)

The calculated values of the $PLI_{site}$ and $PLI_{zone}$ in the study area are shown in **Figure 5**. Both *PLI* values for the site and zone ($PLI_{zone}$=0.52) were below 1, which indicated that the study area was unpolluted.

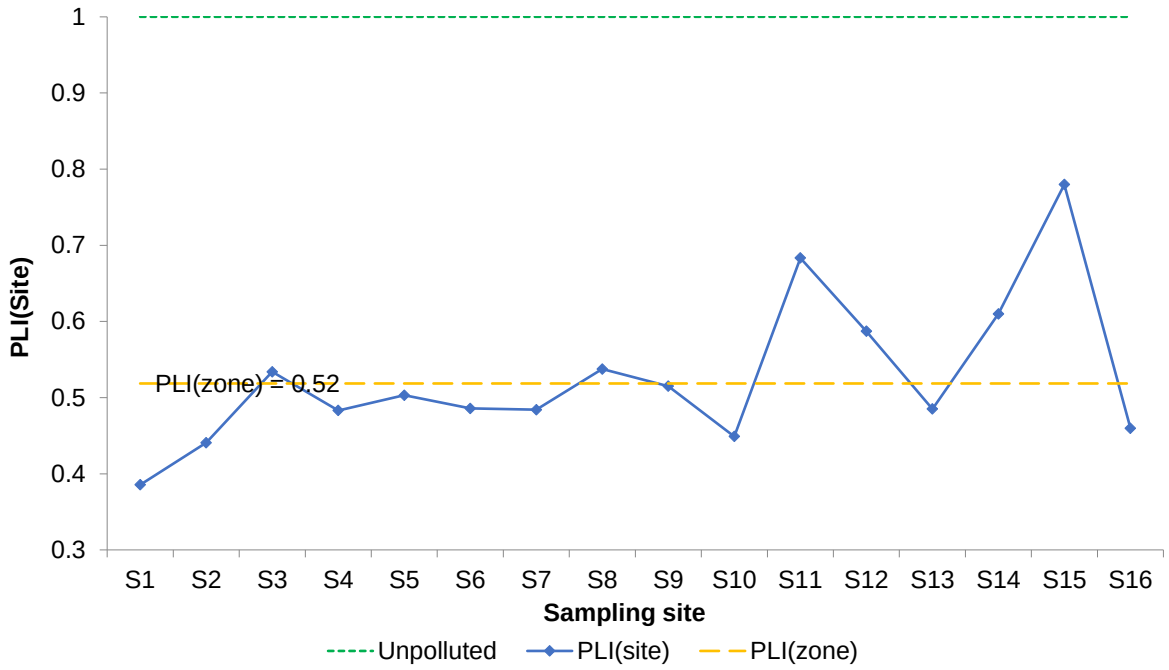


**Fig. 5** Pollution load indexes for the dust samples in the study area

## 2.4 Risk Assessment

### 2.4.1 Ecological risk assessment

The distribution of *ERI* calculated using the Hakanson method in all selected schools in the Ma'an district and the mean percent contribution of *PTE*s to *ERF* are shown in Fig. (6). The contribution of *PTE*s to *ERF* was in the following order: Pb(43%)>Cu (26%)>Zn(17%)>Cr(9%)>V(3%)>Mn=Ni (1%). Similar results were obtained by Yesilkanat and Kobya (2021). The *ERI* values ranged from 10 to 18 indicating very low potential ecological risk (*ERI*<150).

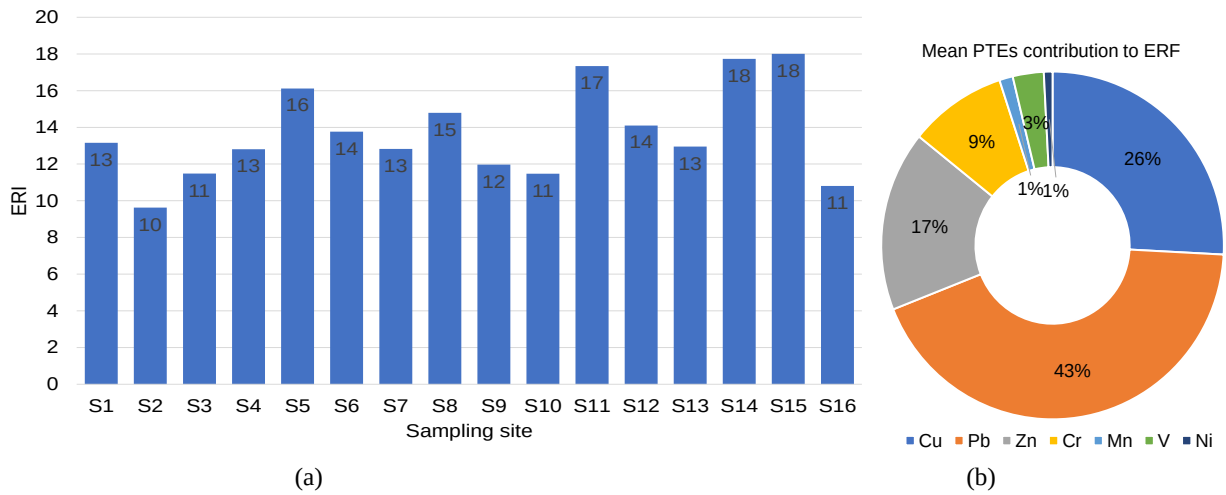


(a) (b)

**Fig. 6** Potential ecological risk results: (a) Distribution of *ERI* in all sampling sites, (b) Mean percent contribution of *PTE*s to *ERF*.

**Table 7** Health risk assessment results of fallout dust by children and adults

| Element | | Al | Cu | Fe | Mn | Ni | Pb | Sr | Zn | |
|---|---|---|---|---|---|---|---|---|---|---|
| $RfD_{ing}$ (mg/kg body weight per day) | | 1.00E+00 | 4.00E-02 | 7.00E-01 | 1.40E-01 | 1.10E-02 | 3.50E-03 | 6.00E-01 | 3.00E-01 | |
| $RfD_{derm}$ (mg/kg body weight per day) | | – | 1.20E-02 | – | – | – | 5.25E-04 | – | 6.00E-01 | |
| $RfD_{inh}$ (mg/m$^3$) | | – | – | – | 5.00E-05 | 1.40E-05 | – | – | – | |
| GIABS | | – | 1.00E+00 | – | – | – | 1.00E+00 | – | 1.00E+00 | |
| *SF* (kg body per day/mg) | | – | – | – | – | 9.00E-01 | 4.20E-02 | – | – | |
| *IUR* (µg/m$^3$)$^{-1}$ | | – | – | – | – | 2.40E-04 | 1.20E-05 | – | – | |
| Mean concentrations (mg/kg) | | 4189.59 | 45.26 | 10127.36 | 191.43 | 2.68 | 11.62 | 206.87 | 160.57 | |
| Non-carcinogenic health risk | | | | | | | | | | HI |
| Children | $ADD_{ing}$ | 1.38E-02 | 1.49E-04 | 3.33E-02 | 6.29E-04 | 8.81E-06 | 3.82E-05 | 6.80E-04 | 5.28E-04 | |
| | $HQI_{ing}$ | 1.38E-02 | 3.72E-03 | 4.76E-02 | 4.50E-03 | 8.01E-04 | 1.09E-02 | 1.13E-03 | 1.76E-03 | **8.42E-02** |
| | $ADD_{derm}$ | 6.43E-05 | 6.94E-07 | 1.55E-04 | 2.94E-06 | 4.11E-08 | 1.78E-07 | 3.17E-06 | 2.46E-06 | |
| | $HQI_{derm}$ | – | 5.79E-05 | – | – | – | 3.40E-04 | – | 4.11E-06 | **4.02E-04** |
| | $ADD_{inh}$ | 1.01E-06 | 1.09E-08 | 2.45E-06 | 4.62E-08 | 6.47E-10 | 2.81E-09 | 5.00E-08 | 3.88E-08 | |
| | $HQI_{inh}$ | – | – | – | 9.25E-07 | 4.62E-08 | – | – | – | **9.71E-07** |
| Adults | $ADD_{ing}$ | 1.48E-03 | 1.59E-05 | 3.57E-03 | 6.74E-05 | 9.43E-07 | 4.09E-06 | 7.29E-05 | 5.66E-05 | |
| | $HQI_{ing}$ | 1.48E-03 | 3.99E-04 | 5.10E-03 | 4.82E-04 | 8.58E-05 | 1.17E-03 | 1.21E-04 | 1.89E-04 | **9.02E-03** |
| | $ADD_{derm}$ | 4.58E-04 | 4.95E-06 | 1.11E-03 | 2.09E-05 | 2.93E-07 | 1.27E-06 | 2.26E-05 | 1.76E-05 | |
| | $HQI_{derm}$ | | 4.13E-04 | – | – | – | 2.42E-03 | – | 2.93E-05 | **1.75E-06** |
| | $ADD_{inh}$ | 4.32E-07 | 4.67E-09 | 1.05E-06 | 1.98E-08 | 2.76E-10 | 1.20E-09 | 2.14E-08 | 1.66E-08 | |
| | $HQI_{inh}$ | – | – | – | 3.95E-07 | 1.97E-08 | – | – | – | **4.15E-07** |
| Carcinogenic health risk | | | | | | | | | | ∑CR |
| Children | $CR_{ing}$ | – | – | – | – | 7.92E-06 | 1.60E-06 | – | – | **9.53E-06** |
| | $CR_{derm}$ | – | – | – | – | – | 4.26E-06 | – | – | **4.26E-06** |
| | $CR_{inh}$ | – | – | – | – | 6.47E-10 | 2.81E-09 | – | – | **3.45E-09** |
| | ***CRisk*** | **1.38E-05** | | | | | | | | |
| Adults | $CR_{ing}$ | – | – | – | – | 8.49E-07 | 1.72E-07 | – | – | **1.02E-06** |
| | $CR_{derm}$ | – | – | – | – | – | 3.02E-05 | – | – | **3.02E-05** |
| | $CR_{inh}$ | – | – | – | – | 6.63E-14 | 1.44E-14 | – | – | **8.07E-14** |
| | ***CRisk*** | **3.13E-05** | | | | | | | | |

No non-carcinogenic health risk  Non-carcinogenic health risk

Very low cancer risk  Low cancer risk  Moderate cancer risk  High cancer risk  Very high cancer risk

### 2.4.2 Health risk assessment

In this study, the health risks of *PTE*s in fallout dust for both children and adults were assessed for carcinogenic and non-carcinogenic potential health risks via dermal contact, inhalation, and ingestion exposure pathways. **Table 7** lists the health risk assessment results of fallout dust by children and adults. The results of the Hazard Quotient (*HQ*I) indicate that oral ingestion is the primary exposure pathway for children and adults. These results were in good agreement with other studies (Shabbaj *et al.,* 2018; Shao *et al.,* 2018; X. Wei *et al.,* 2015). For children, the $HQI_{ing}$ is 3 to 4 orders of magnitude higher than $HQI_{derm}$ and $HQI_{derm}$ is 1 to 2 orders of magnitude higher than $HQI_{inh}$. For adults, the $HQI_{ing}$ is in the same order of magnitude or one order of magnitude higher than $HQI_{derm}$ and $HQI_{derm}$ is 3 orders of magnitude higher than $HQI_{inh}$. The non-carcinogenic hazard index values indicate a similar trend as *HQI* regarding the three exposure pathways: $HI_{ing}>HI_{derm}>HI_{inh}$. *HI*, values for children are higher than adults; $HI_{ing}$ ($8.42x10^{-2}$) for children is one order of magnitude higher than $HI_{ing}$ ($9.02x10^{-3}$) for adults, $HI_{derm}$ ($4.02x10^{-4}$) for children is two orders of magnitude higher than $HI_{derm}$ ($1.75x10^{-6}$) for adults, while $HI_{inh}$ ($HI_{inh,ch}=9.71\times10^{-7}$ and $HI_{inh,ad}=4.15\times10^{-7}$) is in the same order of magnitude. This trend indicates that children's health is more affected by *PTE*s than adults. In this way, *HI* values are lower than one for both children and adults indicating that the school roofs would not cause non-cancer risk (USEPA 1989, 2002). The *HQ* values for each heavy metal are also lower than one, which means there was no non-carcinogenic risk for both children and adults regarding each considered *PTE*s.

The carcinogenic risk values of Ni and Pb were calculated and tabulated in Table 7 for both children and adults. The CR of Ni is higher than Pb for both children and adults during the ingestion pathway. The total CR during ingestion is higher than dermal contact and inhalation for both children and adults indicating that ingestion is the most dangerous pathway. The total CR for children is higher than for adults during both ingestion and dermal contact, which means that children are more exposed to be affected, even though the values are in the range ($1\times10^{-4}$-$1\times10^{-6}$) indicating low cancer risk for both children and adults. During the inhalation pathway, the cancer risk was found to be very low ($CR_{inh}=3.45\times10^{-9}$ for children and $CR_{inh}=8.07\times10^{-14}$ for adults). The integrated carcinogenic risk $CR_{risk}$ for children ($1.38\times10^{-5}$) is lower than for adults ($3.13\times10^{-5}$**)** and they indicate low cancer risk. Yesilkanat and Kobya (2021) found similar results; they found that the averages of the CR total are in the order of Cr>Ni>Pb>Cd for children and adults. They also found that the mean values of HI and TCR are in the negligible noncarcinogenic health risk (*HI*<1) and the lower cancer risk range ($1\times10^{-6}<TCR\leq1\times10^{-4}$) for children and adults.

## Conclusion

The ecological and human health risks of *PTE*s have been successfully assessed for the Ma'an district in Jordan. Dust samples were collected from 16 schools. The XRD patterns showed that all dust samples, with a grain-size fraction <38μm, mainly contain carbonate and silicate minerals (*i.e.* calcite and quartz) with traces of clinoferrosilite and clay mineral (dickite). Among the eight elements studied (Fe, Cu, Pb, Zn, Cr, Mn, V and Ni), the average concentration of Fe was the highest. The mean concentrations of these *PTE*s in the fallout dust are Fe (10127.4mg/kg)>Mn(191.4mg/kg)>Zn(160.6mg/kg)> Cu(42.4mg/kg)>V(35.0mg/kg)>Cr (34.7 mg/kg)>Pb(11.8mg/kg)>Ni(0.7mg/kg). The average concentrations of Fe, Cu, Cr, Mn, V and Ni in the analysed samples were lower than earth crust content, whereas the concentrations of Pb and Zn were 1.20 and 2.30 times higher, respectively. The geochemical indices such as *EF*, *Igeo*, *CF* and *NIPI* for the concerned *PTE*s were in the order of Zn>Pb>Cu>Cr>V>Mn>Ni. However, the $ERF_i$ was in the order Pb>Cu>Zn>Cr>V>Mn>Ni. Based on these geo-chemical indices Zn, Pb and Cu could be considered as the most important pollutants in the study area. The *EF* reveals that the fallout dust deposits were significantly polluted by Zn (12.9) and Pb (6.8), and moderately polluted by Cu (4.1) and Cr (3.7). The *PLI* values (site and zone) were lower than one; indicating that the Ma'an area is not polluted, and the *ERI* values were in the range (10-18) specifying very low potential ecological risk. There was no non-carcinogenic risk for both children and adults regarding each considered *PTE*s since their *HQ* values were lower than one. The *HI* and total *CR* show that ingestion was the most dangerous exposure pathway. The carcinogenic risk values of Ni were higher than Pb for both children and adults during the ingestion pathway. The total *CR* values were in the range between $10^{-4}$ and $10^{-6}$, which indicates low cancer risk for both children and adults. Children could be more affected since the total *CR* for them is higher than for adults during both ingestion and dermal contact. The findings of this paper provide baseline information to authority regarding *PTE* concentration, characterization, and exposure effect on children and adults in the Ma'an district, Jordan. The findings suggest further study for the variability in dust composition across different seasons in Ma'an.

## Nomenclature

| | | |
|---|---|---|
| ABS | =Dermal absorption factor | [-] |
| *ADD* | =Average daily intake dose of *PTE*s affecting both children and adults | [mg/kg-day] |
| *AT* | =Average exposure time | [day] |
| $B_i$ | =Crustal average background concentration of the heavy metal | [mg/kg] |
| *BW* | =Average body weight | [kg] |
| *CF* | =Contamination factor | [-] |
| $C_i$ | =Concentrations of heavy metal in dust sample | [mg/kg] |
| *CR* | =Carcinogenic risk | [-] |
| $C_R$ | =Background concentration of earth crust reference metal | [mg/kg] |
| *CRisk* | =Integrated cancer risk | [-] |
| *ED* | =Exposure duration | [year] |
| *EF* | =Enrichment factor | [-] |
| *EF* | =Exposure frequency | [days/year] |
| *ERF* | =Ecological risk factor | [-] |
| *ERI* | =Ecological risk index | [-] |
| *GIABS* | =Gastrointestinal absorption factor | [-] |
| *HI* | =Hazard index | [-] |
| HMs | =Heavy metals | [-] |
| *HQ* | =Hazard quotient | [-] |
| $I_{geo}$ | =Index of geo-accumulation | [-] |
| *IngR* | =Ingestion rate of dust | [mg/day] |
| *InhR* | =Inhalation rate of dust | [$m^3$/day] |
| *IUR* | =Inhalation unit risk | [1/(μg/$m^3$)] |
| *m* | =Number of sites considered | [-] |
| *n* | =Number of species considered | [-] |
| *NIPI* | =Nemerow Integrated Pollution Index | [-] |
| *PEF* | =Partical emission factor | [$m^3$/kg] |
| *PLI* | =Pollution load index | [-] |
| *PTEs* | =Potentially toxic elements | [-] |
| $RfD_{derm}$ | =Dermal reference dose | [mg/kg-day] |
| $RfD_{ing}$ | =Oral reference dose | [mg/kg-day] |
| $RfD_{inh}$ | =Inhalation reference concentration | [mg/$m^3$], |
| *SA* | =Surface area of exposed skin | [$cm^2$] |
| *SF* | =Slope factor | [kg body per day/mg] |
| *SL* | =Skin adherence factor of dust | [mg/$cm^2$-h] |
| *TR* | =Toxic-response factor | [-] |
| XRD | =X-ray diffraction | [-] |
| XRF | =X-ray fluorescence | [-] |

## References


Adamiec, E., and E., Jarosz-Krzemińska "Human Health Risk Assessment associated with contaminants in the finest fraction of sidewalk dust collected in proximity to trafficked roads", *Scientific Reports*, **9**, 1–11, (2019).

Adimalla, N. "Heavy metals contamination in urban surface soils of Medak province, India, and its risk assessment and spatial distribution", *Env. Geochemistry and Health*, **42**, 59–75, (2020).

Al-Dabbas, M. A., Ayad Abbas, M., and R. M., Al-Khafaji "Dust storms load analyses Iraq", *Arabian J. of Geosciences*, **5**, 121–131, (2012).

Al-Makhadmeh, L. A., Batiha, M. A., Maier, J., Rawadieh, S. E., Altarawneh, I. S., and G., Scheffknecht "Effect of air and oxyfuel staged combustion on oil shale fly ash formation with direct in-furnace limestone addition for sulphur retention", *Fuel*, **220**, 192-199, (2018).

Al-makhadmeh, L. A., Maier, J., Batiha, M., and G., Scheffknecht Oxyfuel technology: Oil shale desulfurization behaviour during staged combustion. *Fuel*, **190**, 226-236, (2017).

Alsbou, E. M. E., and O. A., Al-Khashman "Heavy metal concentrations in roadside soil and street dust from Petra region, Jordan", *Env. Monitoring and Assessment*, **190**, 1–13, (2018).

Amato, F., Cassee, F. R., van der Gon, H. A. C. D., Gehrig, R., Gustafsson, M., Hafner, W., *et al.*, "Urban air quality: the challenge of traffic non-exhaust emissions", *J.of Haz. Mat.*, **275**, 31–36, (2014).

Awadh, S. M. "Geochemistry and mineralogical composition of the airborne particles of sand dunes and dust storms settled in Iraq and their environmental impacts", *Env. Earth Sci.*, **66**, 2247–2256, (2012).

Baensch-Baltruschat, B., Kocher, B., Stock, F., and G., Reifferscheid "Tyre and road wear particles (TRWP) - A review of generation, properties, emissions, human health risk, ecotoxicity, and fate in the environment", *Sci. of the Total Env.*, **733**, 137823, (2020).

Banat, K. M., Howari, F. M., and A. A., Al-Hamad "Heavy metals in urban soils of central Jordan: Should we worry about their environmental risks?", *Env.*

*Res.*, **97**, 258–273, (2005).

Boyle, K. A. "Evaluating particulate emissions from jet engines: analysis of chemical and physical characteristics and potential impacts on coastal environments and human health", *Transportation Res. Record*, **1517**, 1–9, (1996).

Chen, H., Lu, X., Li, L. Y., Gao, T., and Y., Chang "Metal contamination in campus dust of Xi'an, China: A study based on multivariate statistics and spatial distribution", *Sci. of the Total Env.*, **484**, 27–35, (2014).

Chen, Y., Jiang, X., Wang, Y., and D., Zhuang "Spatial characteristics of heavy metal pollution and the potential ecological risk of a typical mining area: A case study in China", *Process Safety and Env. Prot.*, **113**, 204–219, (2018).

Cheng, J. liang, Shi, Z., and Y.wei, Zhu, "Assessment and mapping of environmental quality in agricultural soils of Zhejiang Province, China", *J. of Env. Sci.*, **19**, 50–54, (2007).

Colomban, P., Cherifi, S., andG., Despert "Raman identification of corrosion products on automotive galvanized steel sheets", *J. of Raman Spectroscopy: An Int. J. for Original Work in all Aspects of Raman Spectroscopy, Including Higher Order Processes, and also Brillouin and Rayleigh Scattering*, **39**, 881–886, (2008).

Dallwitz, W. B., Green, D. H., and J. E., Thompson "Clinoenstatite in a volcanic rock from the Cape Vogel area, Papua", *J. of Petrology*, **7**, 375–403, (1966).

De Groot, A. J., Zschuppel, K. H., and W., Salomons "Standardization of methods of analysis for heavy metals in sediments", *Hydrobiologia*, **91**, 689–695, (1982).

El-Radaideh, N. M., and A. A., Al-Taani "Geo-environmental study of heavy metals of the agricultural highway soils, NW Jordan", *Arabian J. of Geosciences*, **11**, 787, (2018).

Ferreira-Baptista, L., and E., De Miguel "Geochemistry and risk assessment of street dust in Luanda, Angola: A tropical urban environment", *Atmospheric Env.*, **39**, 4501–4512, (2005).

Ganor, E., and H. A., Foner "The mineralogical and chemical properties and the behaviour of aeolian Saharan dust over Israel", In *The impact of desert dust across the Mediterranean*, 163–172, Springer, (1996).

Ghrefat, H. A., Yusuf, N., Jamarh, A., and J., Nazzal "Fractionation and risk assessment of heavy metals in soil samples collected along Zerqa River, Jordan", *Env. Earth Sci.*, **66**, 199–208, (2012).

Gope, M., Masto, R. E., George, J., Hoque, R. R., and S., Balachandran "Bioavailability and health risk of some potentially toxic elements (Cd, Cu, Pb and Zn) in street dust of Asansol, India", *Ecotoxicology and Env. Safety*, **138**, 231–241, (2017).

Hakanson, L. "An ecological risk index for aquatic pollution control a sedimentological approach", *Water Res.*, **14**, 975–1001, (1980).

Hamaiedh, H., and T., El-Hasan "Inorganic chemistry, granulometry and mineralogical characteristics of the dust fall over phosphate mine adjacent area, central Jordan", *Env. Earth Sci.*, **62**, 1771–1777, (2011).

He, D., Shi, X., and D., Wu"Particle-size distribution characteristics and pollution of heavy metals in the surface sediments of Kuitun River in Xinjiang, China", *Env. Earth Sci.*, **75**, 1–10, (2016).

Hojati, S., Khademi, H., Faz Cano, A., and A., Landi "Characteristics of dust deposited along a transect between central Iran and the Zagros Mountains", *Catena*, **88**, 27–36, (2012).

Horowitz, A. J., and K. A., Elrick "An evaluation of air elutriation for sediment particle size separation and subsequent chemical analysis", *Env. Tech.*, **7**, 17–26, (1986).

Idris, A. M., Eltayeb, M. A. H., Potgieter-Vermaak, S. S., Van Grieken, R., and J. H., Potgieter "Assessment of heavy metals pollution in Sudanese harbours along the Red Sea Coast", *Microchemical J.*, **87**, 104–112, (2007).

Jaishankar, M., Tseten, T., Anbalagan, N., Mathew, B. B., and K. N., Beeregowda "Toxicity, mechanism and health effects of some heavy metals", *Interdisciplinary Toxicology*, **7**, 60, (2014).

Jayarathne, A., Egodawatta, P., Ayoko, G. A., and A., Goonetilleke "Assessment of ecological and human health risks of metals in urban road dust based on geochemical fractionation and potential bioavailability", *Sci. of the Total Env.*, **635**, 1609–1619, (2018).

Jordanova, N., Jordanova, D., Tcherkezova, E., Georgieva, B., and D., Ishlyamski "Advanced mineral magnetic and geochemical investigations of road dust for assessment of pollution in urban areas near the largest copper smelter in SE Europe", *Sci. of the Total Env.*, **792**, 148402, (2021).

Khlifi, R., Olmedo, P., Gil, F., Hammami, B., Chakroun, A., Rebai, A., and A., Hamza-Chaffai "Arsenic, cadmium, chromium and nickel in cancerous and healthy tissues from patients with head and neck cancer", *Sci. of the Total Env.*, **452**, 58–67, (2013).

Kirpichtchikova, T. A., Manceau, A., Spadini, L., Panfili, F., Marcus, M. A., and T., Jacquet"Speciation and solubility of heavy metals in contaminated soil using X-ray microfluorescence, EXAFS spectroscopy, chemical extraction, and thermodynamic modelling", *Geochimica et Cosmochimica Acta*, **70**, 2163–2190, (2006).

Lee, J. H., and P. K., Hopke "Apportioning sources of PM2. 5 in St. Louis, MO using speciation trends network data" *Atmospheric Env.*, **40**, 360–377, (2006).

Li, H. H., Chen, L. J., Yu, L., Guo, Z. B., Shan, C. Q., Lin, J. Q., *et al.*, "Pollution characteristics and risk assessment of human exposure to oral bioaccessibility of heavy metals via urban street dust from different functional areas in Chengdu, China", *Sci. of the Total Env.*, **586**, 1076–1084, (2017).

Li, X., Poon, C., and P. S., Liu "Heavy metal contamination of urban soils and street dusts in Hong Kong", *Appl. Geochemistry*, **16**, 1361–1368, (2001).

Li, Y., Yu, Y., Yang, Z., Shen, Z., Wang, X., and Y., Cai "A comparison of metal distribution in surface dust and soil among super city, town, and rural area", *Env. Sci. and Pollution Res.*, **23**, 7849–7860, (2016).

Loska, K., Wiechuła, D., and I., Korus "Metal contamination of farming soils affected by industry", *Env. Int.*, **30**, 159–165, (2004).

Manno, E., Varrica, D., and G., Dongarra "Metal distribution in road dust samples collected in an urban area close to a petrochemical plant at Gela, Sicily", *Atmospheric Env.*, **40**, 5929–5941, (2006).

Mason, B. J. "Ice-nucleating properties of clay minerals and stony meteorites", *Quarterly J. of the Royal Meteorological Soc.*, **86**, 552–556, (1960).

Men, C., Liu, R., Wang, Q., Guo, L., and Z., Shen "The impact of seasonal varied human activity on characteristics and sources of heavy metals in metropolitan road dusts", *Sci. of the Total Env.*, **637–638**, 844–854, (2018).

Merefield, J., Stone, I., Jarman, P., Rees, G., Roberts, J., Jones, J., and A., Dean "Environmental dust analysis in opencast mining areas", *Geological Soc. Special Publication*, **82**, 181–188, (1995).

Modaihsh, A., Ghoneim, A., Al-Barakah, F., Mahjoub, M., and M., Nadeem "Characterizations of deposited dust fallout in Riyadh city, Saudi Arabia", *Polish J. of Env. Stud.*, **26**, 1599–1605, (2017).

Muller, G. "Index of geoaccumulation in sediments of the Rhine River", *Geojournal*, **2**, 108–118, (1969).

Najafi, M. S., Khoshakhllagh, F., Zamanzadeh, S. M., Shirazi, M. H., Samadi, M., and S., Hajikhani "Characteristics of TSP Loads during the Middle East Springtime Dust Storm (MESDS) in Western Iran", *Arabian J. of Geosciences*, **7**, 5367–5381, (2014).

Pal, S. K., and R., Roy |"Evaluating heavy metals emission' pattern on road influenced by urban road layout", *Transportation Res. Interdisciplinary Perspectives*, **10**, 100362, (2021).

Pan, H., Lu, X., and K., Lei "A comprehensive analysis of heavy metals in urban road dust of Xi'an, China: Contamination, source apportionment and spatial distribution", *Sci. of the Total Env.*, **609**, 1361–1369, (2017).

Adamiec, E., and E., Jarosz-Krzemińska "Human Health Risk Assessment associated with contaminants in the finest fraction of sidewalk dust collected in proximity to trafficked roads", *Scientific Reports*, **9**, 1–11, (2019).

Adimalla, N. "Heavy metals contamination in urban surface soils of Medak province, India, and its risk assessment and spatial distribution", *Env. Geochemistry and Health*, **42**, 59–75, (2020).

Al-Dabbas, M. A., Ayad Abbas, M., and R. M., Al-Khafaji "Dust storms loads analyses Iraq", *Arabian J. of Geosciences*, **5**, 121–131, (2012).

Al-Makhadmeh, L. A., Batiha, M. A., Maier, J., Rawadieh, S. E., Altarawneh, I. S., and G., Scheffknecht "Effect of air and oxyfuel staged combustion on oil shale fly ash formation with direct in-furnace limestone addition for sulphur retention", *Fuel*, **220**, 192-199, (2018).

Al-makhadmeh, L. A., Maier, J., Batiha, M., and G., Scheffknecht Oxyfuel technology: Oil shale desulfurization behavior during staged combustion. *Fuel*, **190**, 226-236, (2017).

Alsbou, E. M. E., and O. A., Al-Khashman "Heavy metal concentrations in roadside soil and street dust from Petra region, Jordan", *Env. Monitoring and Assessment*, **190**, 1–13, (2018).

Amato, F., Cassee, F. R., van der Gon, H. A. C. D., Gehrig, R., Gustafsson, M., Hafner, W., *et al.*, "Urban air quality: the challenge of traffic non-exhaust emissions", *J.of Haz. Mat.*, **275**, 31–36, (2014).

Awadh, S. M. "Geochemistry and mineralogical composition of the airborne particles of sand dunes and dust storms settled in Iraq and their environmental impacts", *Env. Earth Sci.*, **66**, 2247–2256, (2012).

Baensch-Baltruschat, B., Kocher, B., Stock, F., and G., Reifferscheid "Tyre and road wear particles (TRWP) - A review of generation, properties, emissions, human health risk, ecotoxicity, and fate in the environment", *Sci. of the Total Env.*, **733**, 137823, (2020).

Banat, K. M., Howari, F. M., and A. A., Al-Hamad "Heavy metals in urban soils of central Jordan: Should we worry about their environmental risks?", *Env. Res.*, **97**, 258–273, (2005).

Boyle, K. A. "Evaluating particulate emissions from jet engines: analysis of chemical and physical characteristics and potential impacts on coastal environments and human health", *Transportation Res. Record*, **1517**, 1–9, (1996).

Chen, H., Lu, X., Li, L. Y., Gao, T., and Y., Chang "Metal contamination in campus dust of Xi'an, China: A study based on multivariate statistics and spatial distribution", *Sci. of the Total Env.*, **484**, 27–35, (2014).

Chen, Y., Jiang, X., Wang, Y., and D., Zhuang "Spatial characteristics of heavy metal pollution and the potential ecological risk of a typical mining area: A case study in China", *Process Safety and Env. Prot.*, **113**, 204–219, (2018).

Cheng, J. liang, Shi, Z., and Y.wei, Zhu, "Assessment and mapping of environmental quality in agricultural soils of Zhejiang Province, China", *J. of Env. Sci.*, **19**, 50–54, (2007).

Colomban, P., Cherifi, S., andG., Despert "Raman identification of corrosion products on automotive galvanized steel sheets", *J. of Raman Spectroscopy: An Int. J. for Original Work in all Aspects of Raman Spectroscopy, Including Higher Order Processes, and also Brillouin and Rayleigh Scattering*, **39**, 881–886, (2008).

Dallwitz, W. B., Green, D. H., and J. E., Thompson "Clinoenstatite in a volcanic rock from the Cape Vogel area, Papua", *J. of Petrology*, **7**, 375–403, (1966).

De Groot, A. J., Zschuppel, K. H., and W., Salomons "Standardization of methods of analysis for heavy metals in sediments", *Hydrobiologia*, **91**, 689–695, (1982).

El-Radaideh, N. M., and A. A., Al-Taani "Geo-environmental study of heavy metals of the agricultural highway soils, NW Jordan", *Arabian J. of Geosciences*, **11**, 787, (2018).

Ferreira-Baptista, L., and E., De Miguel "Geochemistry and risk assessment of street dust in Luanda, Angola: A tropical urban environment", *Atmospheric Env.*, **39**, 4501–4512, (2005).

Ganor, E., and H. A., Foner "The mineralogical and chemical properties and the behaviour of aeolian Saharan dust over Israel", In *The impact of desert dust across the Mediterranean*, 163–172, Springer, (1996).

Ghrefat, H. A., Yusuf, N., Jamarh, A., and J., Nazzal "Fractionation and risk assessment of heavy metals in soil samples collected along Zerqa River, Jordan", *Env. Earth Sci.*, **66**, 199–208, (2012).

Gope, M., Masto, R. E., George, J., Hoque, R. R., and S., Balachandran "Bioavailability and health risk of some potentially toxic elements (Cd, Cu, Pb and Zn) in street dust of Asansol, India", *Ecotoxicology and Env. Safety*, **138**, 231–241, (2017).

Hakanson, L. "An ecological risk index for aquatic pollution control a sedimentological approach", *Water Res.*, **14**, 975–1001, (1980).

Hamaiedh, H., and T., El-Hasan "Inorganic chemistry, granulometry and mineralogical characteristics of the dust fall over phosphate mine adjacent area, central Jordan", *Env. Earth Sci.*, **62**, 1771–1777, (2011).

He, D., Shi, X., and D., Wu"Particle-size distribution characteristics and pollution of heavy metals in the surface sediments of Kuitun River in Xinjiang, China", *Env. Earth Sci.*, **75**, 1–10, (2016).

Hojati, S., Khademi, H., Faz Cano, A., and A., Landi "Characteristics of dust deposited along a transect between central Iran and the Zagros Mountains", *Catena*, **88**, 27–36, (2012).

Horowitz, A. J., and K. A., Elrick "An evaluation of air elutriation for sediment particle size separation and subsequent chemical analysis", *Env. Tech.*, **7**, 17–26, (1986).

Idris, A. M., Eltayeb, M. A. H., Potgieter-Vermaak, S. S., Van Grieken, R., and J. H., Potgieter "Assessment of heavy metals pollution in Sudanese harbours along the Red Sea Coast", *Microchemical J.*, **87**, 104–112, (2007).

Jaishankar, M., Tseten, T., Anbalagan, N., Mathew, B. B., and K. N., Beeregowda "Toxicity, mechanism and health effects of some heavy metals", *Interdisciplinary Toxicology*, **7**, 60, (2014).

Jayarathne, A., Egodawatta, P., Ayoko, G. A., and A., Goonetilleke "Assessment of ecological and human health risks of metals in urban road dust based on geochemical fractionation and potential bioavailability", *Sci. of the Total Env.*, **635**, 1609–1619, (2018).

Jordanova, N., Jordanova, D., Tcherkezova, E., Georgieva, B., and D., Ishlyamski "Advanced mineral magnetic and geochemical investigations of road dusts for assessment of pollution in urban areas near the largest copper smelter in SE Europe", *Sci. of the Total Env.*, **792**, 148402, (2021).

Khlifi, R., Olmedo, P., Gil, F., Hammami, B., Chakroun, A., Rebai, A., and A., Hamza-Chaffai "Arsenic, cadmium, chromium and nickel in cancerous and healthy tissues from patients with head and neck cancer", *Sci. of the Total Env.*, **452**, 58–67, (2013).

Kirpichtchikova, T. A., Manceau, A., Spadini, L., Panfili, F., Marcus, M. A., and T., Jacquet"Speciation and solubility of heavy metals in contaminated soil using X-ray microfluorescence, EXAFS spectroscopy, chemical extraction, and thermodynamic modeling", *Geochimica et Cosmochimica Acta*, **70**, 2163–2190, (2006).

Lee, J. H., and P. K., Hopke "Apportioning sources of PM2. 5 in St. Louis, MO using speciation trends network data" *Atmospheric Env.*, **40**, 360–377, (2006).

Li, H. H., Chen, L. J., Yu, L., Guo, Z. B., Shan, C. Q., Lin, J. Q., *et al.*, "Pollution characteristics and risk assessment of human exposure to oral bioaccessibility of heavy metals via urban street dusts from different functional areas in Chengdu, China", *Sci. of the Total Env.*, **586**, 1076–1084, (2017).

Li, X., Poon, C., and P. S., Liu "Heavy metal contamination of urban soils and street dusts in Hong Kong", *Appl. Geochemistry*, **16**, 1361–1368, (2001).

Li, Y., Yu, Y., Yang, Z., Shen, Z., Wang, X., and Y., Cai "A comparison of metal distribution in surface dust and soil among super city, town, and rural area", *Env. Sci. and Pollution Res.*, **23**, 7849–7860, (2016).

Loska, K., Wiechułła, D., and I., Korus "Metal contamination of farming soils affected by industry", *Env. Int.*, **30**, 159–165, (2004).

Manno, E., Varrica, D., and G., Dongarra "Metal distribution in road dust samples collected in an urban area close to a petrochemical plant at Gela, Sicily", *Atmospheric Env.*, **40**, 5929–5941, (2006).

Mason, B. J. "Ice-nucleating properties of clay minerals and stony meteorites", *Quarterly J. of the Royal Meteorological Soc.*, **86**, 552–556, (1960).

Men, C., Liu, R., Wang, Q., Guo, L., and Z., Shen "The impact of seasonal varied human activity on characteristics and sources of heavy metals in metropolitan road dusts", *Sci. of the Total Env.*, **637–638**, 844–854, (2018).

Merefield, J., Stone, I., Jarman, P., Rees, G., Roberts, J., Jones, J., and A., Dean "Environmental dust analysis in opencast mining areas", *Geological Soc. Special Publication*, **82**, 181–188, (1995).

Modaihsh, A., Ghoneim, A., Al-Barakah, F., Mahjoub, M., and M., Nadeem "Characterizations of deposited dust fallout in Riyadh city, Saudi Arabia", *Polish J. of Env. Stud.*, **26**, 1599–1605, (2017).

Muller, G. "Index of geoaccumulation in sediments of the Rhine River", *Geojournal*, **2**, 108–118, (1969).

Najafi, M. S., Khoshakhllagh, F., Zamanzadeh, S. M., Shirazi, M. H., Samadi, M., and S., Hajikhani "Characteristics of TSP Loads during the Middle East Springtime Dust Storm (MESDS) in Western Iran", *Arabian J. of Geosciences*, **7**, 5367–5381, (2014).

Pal, S. K., and R., Roy |"Evaluating heavy metals emission' pattern on road influenced by urban road layout", *Transportation Res. Interdisciplinary Perspectives*, **10**, 100362, (2021).

Pan, H., Lu, X., and K., Lei "A comprehensive analysis of heavy metals in urban road dust of Xi'an, China: Contamination, source apportionment and spatial distribution", *Sci. of the Total Env.*, **609**, 1361–1369, (2017).

Pant, P., and R. M., Harrison "Estimation of the contribution of road traffic emissions to particulate matter concentrations from field measurements: A review", *Atmospheric Env.*, **77**, 78–97, (2013).

Potgieter-Vermaak, S., Rotondo, G., Novakovic, V., Rollins, S., and R., Van Grieken "Component-specific toxic concerns of the inhalable fraction of urban road dust", *Env. Geochemistry and Health*, **34**, 689–696, (2012).

Pye, K. "Aeolian dust transport and deposition over Crete and adjacent parts of the Mediterranean Sea", *Earth Surface Processes and Landforms*, **17**, 271–288, (1992).

Qadeer, A., Saqib, Z. A., Ajmal, Z., Xing, C., Khan Khalil, S., Usman, M., *et al.*, "Concentrations, pollution indices and health risk assessment of heavy metals in road dust from two urbanized cities of Pakistan: Comparing two sampling methods for heavy metals concentration", *Sustainable Cities and Soc.*, **53**, 101959, (2020).

Rai, P. K. "Impacts of particulate matter pollution on plants: Implications for environmental biomonitoring", *Ecotoxicology and Env. safety*, **129**, 120–136, (2016).

Rashki, A., Eriksson, P. G., Rautenbach, C. J. d. W., Kaskaoutis, D. G., Grote, W., and J., Dykstra "Assessment of chemical and mineralogical characteristics of airborne dust in the Sistan region, Iran", *Chemosphere*, **90**, 227–236, (2013).

Robertson, D. J., and K. G., Taylor "Temporal variability of metal contamination in urban road-deposited sediment in Manchester, UK: Implications for urban pollution monitoring", *Water, Air, and Soil Pollution*, **186**, 209–220, (2007).

Saleem, M., Iqbal, J., Akhter, G., and M. H., Shah "Fractionation, bioavailability, contamination and environmental risk of heavy metals in the sediments from a freshwater reservoir, Pakistan", *J. of Geochemical Exploration*, **184**, 199–208, (2018).

Shabbaj, I. I., Alghamdi, M. A., Shamy, M., Hassan, S. K., Alsharif, M. M., and M. I., Khoder "Risk assessment and implication of human exposure to road dust heavy metals in Jeddah, Saudi Arabia", *Int. J. of Env. Res. and Public Health*, **15**, 36, (2018).

Shaltout, A. A., Allam, M. A., Mostafa, N. Y., and Z. K., Heiba "Spectroscopic Characterization of Dust-Fall Samples Collected from Greater Cairo, Egypt", *Archives of Env.l Contamination and Toxicology*, **70**, 544–555, (2016).

Shao, T., Pan, L., Chen, Z., Wang, R., Li, W., Qin, Q., and Y., He "Content of heavy metal in the dust of leisure squares and its health risk assessment—a case study of Yanta district in Xi'an", *Int. J.l of Env. Res. and Public Health*, **15**, 1–13, (2018).

Singh, A. K. "Elemental chemistry and geochemical partitioning of heavy metals in road dust from Dhanbad and Bokaro regions, India", *Env. Earth Sci.*, **62**, 1447–1459, (2011).

Singh, A. K., Hasnain, S. I., and D. K., Banerjee"Grain size and geochemical partitioning of heavy metals in sediments of the Damodar River–a tributary of the lower Ganga, India", *Env. Geology*, **39**, 90–98, (1999).

Sydbom, A., Blomberg, A., Parnia, S., Stenfors, N., Sandström, T., and S. E., Dahlen "Health effects of diesel exhaust emissions", *European Respiratory J.*, **17**, 733–746, (2001).

Taylor, S R, Mclennan, S. M., Armstrong, R. L., and J., Tarney "The composition and evolution of the continental crust: rare earth element evidence from sedimentary rocks", *Philosophical Transactions of the Royal Soc. of London Series A, Math. and Phy. Sci.*, **301**, 381–399, (1981).

Taylor, Stuart Ross, and S. M., Mclennan "The geochemical the continental evolution crust", *Reviews in Mineralogy and Geochemistry*, **33**, 241–265, (1995).

Tomlinson, D. L., Wilson, J. G., Harris, C. R., and D. W., Jeffrey "Problems in the assessment of heavy-metal levels in estuaries and the formation of a

pollution index", *Helgoländer Meeresuntersuchungen*, **33**, 566–575, (1980).

USEPA *Risk assessment guidance for superfund*. Office of Emergency and Remedial Response, US Environmental Protection Agency, (1989).

USEPA Soil screening guidance: Technical background document Superfund US EPA, (1996). *Washington, DC: US Environmental Protection Agency.[Accessed 7 March 2018]*.

USEPA Tâm Thư Trí Thủ. *Regional Screening Levels (RSLs)—Generic Tables*. https://www.epa.gov/risk/regional-screening-levels-rsls-generic-tables (2001). Accessed 1 November 2021

USEPA Supplemental guidance for developing soil screening levels for superfund sites. OSWER, (2002).

USEPA Estimation of relative bioavailability of lead in soil and soil-like materials using in vivo and in vitro methods. *Washington, DC: US Environmental Protection Agency, Office of Solid Waste and Emergency Response*, (2007).

USEPA Exposure Factors Handbook 2011 Edition (Final). *DC, EPA/600/R-09/052F*, (2011). https://www.nrc.gov/docs/ML1400/ML14007A666.pdf. Accessed 1 November 2021

USEPA, I. Reference Dose (RfD): Description and Use in Health Risk Assessments, Background Document 1A, Integrated Risk Information System (IRIS). *USEPA Washington DC*, (1993).

Wang, S., Wang, L., Huan, Y., Wang, R., and T., Liang "Concentrations, spatial distribution, sources and environmental health risks of potentially toxic elements in urban road dust across China", *Sci. of The Total Env.*, **805**, 150266, (2022).

Wei, B., Jiang, F., Li, X., and S., Mu "Spatial distribution and contamination assessment of heavy metals in urban road dusts from Urumqi, NW China", *Microchemical J.*, **93**, 147–152, (2009).

Wei, B., and L., Yang "A review of heavy metal contaminations in urban soils, urban road dusts and agricultural soils from China", *Microchemical J.*, **94**, 99–107, (2010).

Wei, X., Gao, B., Wang, P., Zhou, H., and J., Lu "Pollution characteristics and health risk assessment of heavy metals in street dusts from different functional areas in Beijing, China", *Ecotoxicology and Env. Safety*, **112**, 186–192, (2015).

Wiseman, C. L. S., Levesque, C., and P. E., Rasmussen "Characterizing the sources, concentrations and resuspension potential of metals and metalloids in the thoracic fraction of urban road dust", *Sci. of the Total Env.*, **786**, 147467, (2021).

Yeats, P. A., and J. M., Bewers "Discharge of metals from the St. Lawrence River", *Canadian J. of Earth Sci.*, **19**, 982–992, (1982).

Yesilkanat, C. M., and Y., Kobya "Spatial characteristics of ecological and health risks of toxic heavy metal pollution from road dust in the Black Sea coast of Turkey", *Geoderma Regional*, **25**, e00388, (2021).

Zarasvandi, A., Carranza, E. J. M., Moore, F., and F., Rastmanesh "Spatio-temporal occurrences and mineralogical-geochemical characteristics of airborne dusts in Khuzestan Province (southwestern Iran)", *J. of Geochemical Exploration*, **111**, 138–151, (2011).

Zhou, Q., Zheng, N., Liu, J., Wang, Y., Sun, C., Liu, Q., *et al*., "Residents health risk of Pb, Cd and Cu exposure to street dust based on different particle sizes around zinc smelting plant, Northeast of China", *Env.Geochemistry and Health*, **37**, 207–220, (2015).

Zoller, W. H., Gladney, E. S., and R. A., Duce "Atmospheric concentrations and sources of trace metals at the South Pole", *Science*, **183**, 198–200, (1974).